Proceedings of the Estonian Academy of Sciences,
2023, **72**, 2, 128–144
https://doi.org/10.3176/proc.2023.2.04
Available online at www.eap.ee/proceedings

OPTICAL SOLITONS

W-shaped chirp free and chirped bright, dark solitons for perturbed nonlinear Schrödinger equation in nonlinear optical fibers

Annamalai Muniyappan[a], Muthuvel Sharmila[a], Elumalai Kaviya Priya[a], Sekar Sumithra[a], Anjan Biswas[b,c,d,e*], Yakup Yıldırım[f,g], Maggie Aphane[e], Seithuti P. Moshokoa[h] and Hashim M. Alshehri[c]

[a] Department of Physics, Theivanai Ammal College for Women (A), Villupuram 605 401, Tamilnadu, India
[b] Department of Mathematics and Physics, Grambling State University, Grambling, LA 71245, USA
[c] Mathematical Modeling and Applied Computation (MMAC) Research Group, Department of Mathematics, King Abdulaziz University, Jeddah 21589, Saudi Arabia
[d] Department of Applied Sciences, Cross–Border Faculty, Dunarea de Jos University of Galati, 111 Domneasca Street, Galati 800201, Romania
[e] Department of Mathematics and Applied Mathematics, Sefako Makgatho Health Sciences University, Medunsa 0204, South Africa
[f] Department of Computer Engineering, Biruni University, Istanbul 34010, Turkey
[g] Department of Mathematics, Near East University, Nicosia 99138, Cyprus
[h] Department of Mathematics and Statistics, Tshwane University of Technology, Pretoria 0008, South Africa

Received 3 September 2022, accepted 3 October 2022, available online 20 March 2023

Abstract. In the present investigation, we employed the Jacobi elliptic function (JEF) method to invoke the perturbed nonlinear Schrödinger equation with self-steepening (SS), self-phase modulation (SPM), and group velocity dispersion (GVD), which govern the propagation of solitonic pulses in optical fibres. The proposed algorithm proves the existence of the family of solitons in optical fibers. Consequently, chirped and chirp free W-shaped bright, dark soliton solutions are obtained from dn(ξ), cn(ξ) and sn(ξ) functions. The final results are displayed in three-dimensional plots with specific physical values of GVD, SPM and SS for an optical fiber.

Keywords: solitons, Jacobi elliptic function method, NLS equation, differential equation.

1. INTRODUCTION

Solitons are nonlinear localized waves that can be found in the field of optics. This is because of the nonlinear reaction of the medium. In the process of considering the nonlinearity of transmitted waves, specifically for solitons, numerous heterogeneous forms of mathematical techniques have been explored. In the most recent few decades, there has been a substantial upsurge in interest surrounding the study of nonlinear wave phenomena such as breather waves, solitons, rogue waves, and many other types of waves. Researchers in the fields of engineering and applied sciences have found that the process of extracting

* Corresponding author, biswas.anjan@gmail.com

solitons with nonlinear partial differential equations (NLPDEs) is one of the most interesting and intriguing subjects to study [3–6]. This result was confirmed by a large number of the scientists and engineers who have worked in these fields. The transmission of digital information across optical fibres is the most significant technological usage of the soliton, and it is accomplished by using this pulse. The remarkable subject of nonlinear optics known as the optical soliton explores a wide range of topics, including birefringent crystals, meta-surfaces, optical couplers, optical fibres, and magneto-optics [7–12].

NLPDEs can be used to model a broad variety of difficult processes that arise in real life and can be applied across many scientific disciplines [1–6]. The phenomenal cosmos is made up of virtually an infinite number of fascinating nonlinear occurrences that act as complementary elements. During the process of mathematical formulation, the nonlinearity of the resulting complex dynamical systems emerges. The nonlinear Schrödinger equation (NLSE) is one of the most important nonlinear evolution equations (NLEEs). The NLSE can be expressed in its most general form as a cubic nonlinearity, which has several applications in the research on waves in optical fibres [9,10]. The complicated forms of higher order with intent special of NLSEs have been prepared with a number of different genera of nonlinear variables. It is common knowledge that the NLSE plays a significant part in a variety of subfields of nonlinear research, including Bose–Einstein condensates [14], nonlinear optics [15–17], and water waves [13]. In particular, the NLSE is able to represent the propagation of a picosecond optical pulse through optical fibres [18].

Recent years have seen an increase in the number of researchers interested in obtaining chirped femtosecond optical pulses for application in communication systems [19–24]. Goyal et al. [19] used self-frequency shift (SFS) and self-steepening (SS) to characterise the chirped brilliant, double-kink, and dark solitons of the cubic-quintic (CQ) NLSE. These solitons are described as having the CQ-NLSE. Bright, kink, and dark solitons with nonlinear chirp are derived for the NLSE having SS and SFS effects [20,21]. Also, higher-order NLSEs with non-Kerr law components are taken into consideration in the process of researching chirped femtosecond optical pulses in optical fibres [22–24]. These chirped solitonic pulses are essential in the design of solitary wave-based communications links, fiber-optic amplifiers, and optical pulse compressors [25]. They have many applications in pulse amplification or compression, and these applications include a wide variety of compression and amplification techniques. The chirped and chirp free W-shaped dark and bright solitonic structures are secured in Section 2 by applying the Jacobi elliptic function (JEF) method. In this research, these findings are given and addressed in Section 3.

2. MODEL DYNAMICAL EQUATION

The governing model to study the influence of self-phase modulation (SPM), dispersion, and SS effects on the propagation dynamics with perturbed NLSE is considered as

$$iu_t + \alpha u_{xx} + \beta |u|^2 u - i\left[\Gamma u_x - \delta(|u|^2 u)_x - \sigma(|u|^2)_x u\right] = 0. \tag{1}$$

In order to solve the problem (1), the wave transformation is organized as

$$\xi = x - ct,\ u(x,t) = u(\xi)\exp\{i(\kappa x - \omega t)\}. \tag{2}$$

Here α, β, Γ, δ, and σ are all constants. Additionally, c, κ, and ω are all considered to be constants. The wave variable is denoted by ξ, the frequency is denoted by κ, the wave number is denoted by ω, and the velocity is denoted by c. In this context, the wave profile of the solitonic structure is denoted by the expression $u = u(x,t)$, while nonlinear dispersion (ND), SS, inter-modal dispersion (IMD), SPM, and group velocity dispersion (GVD) come from the parameters σ, δ, Γ, β, α in sequence. When we combine Eq. (2) with Eq. (1), we get the following:

$$u''(\xi) + A_2 u^3(\xi) + A_1 u(\xi) + i\left[\left(\frac{B_2}{B_1}\right)u'(\xi)u^2(\xi) + u'(\xi)\right] = 0, \tag{3}$$

where $A_1 = \frac{\omega - \alpha\kappa^2 + \Gamma\kappa}{\alpha}$, $A_2 = \frac{\beta - \delta\kappa}{\alpha}$, $B_1 = 2\alpha\kappa - c - \Gamma$, and $B_2 = 3\delta + 2\sigma$.

2.1. Analysis of Jacobi elliptic function (JEF) method

It is imperative that exact solutions to NPDEs are implemented in order to generate influential predictions for further merits related to nature and living. The following are some of the methods that extract solitons with NPDEs: the double exponential function algorithm, the Bäcklund transformation procedure, the modified extended tangent hyperbolic function scheme, the generalised auxiliary equation approach, the (G'/G)-expansion methodology, the homogeneous balance technique, the extended rational sin-cos and sinh-cosh procedure. In recent years, the JEF approach, symbolic computation and other forms of computation [1–25] have been addressed to locate solitons with NLEEs.

The value of the parameter m, expressed as m $(0 < m < 1)$, determines the modulus of JEFs. The JEF procedure will make the functions into hyperbolic versions of themselves for setting $m \to 1$. After setting $m \to 1$, perform the following steps: $\mathrm{dn}(\xi) \to \mathrm{sech}\,(\xi)$, $\mathrm{cn}(\xi) \to \mathrm{sech}(\xi)$, and $\mathrm{sn}\,(\xi) \to \tanh(\xi)$. In addition, these functions turn into trigonometric functions for $m \to 0$. Eq. (3) is adequate to solve the problem

$$u(\xi) = \sum_{i=0}^{n} a_i \mathrm{sn}^i(\xi),\ a_n \neq 0, \tag{4}$$

$$u(\xi) = \sum_{i=0}^{n} a_i \mathrm{cn}^i(\xi),\ a_n \neq 0, \tag{5}$$

$$u(\xi) = \sum_{i=0}^{n} a_i \mathrm{dn}^i(\xi),\ a_n \neq 0, \tag{6}$$

along with

$$\mathrm{dn}'(\xi) = -m^2\mathrm{cn}(\xi)\mathrm{sn}(\xi),\ \mathrm{cn}'(\xi) = -\mathrm{dn}(\xi)\mathrm{sn}(\xi),\ \mathrm{sn}'(\xi) = \mathrm{dn}(\xi)\mathrm{cn}(\xi),$$
$$\mathrm{dn}^2(\xi) = 1 - m^2\mathrm{sn}(\xi),\ \mathrm{cn}^2(\xi) + \mathrm{sn}^2(\xi) = 1.$$

Here n is the number that must be balanced, and a_i $(i = 0, 1, \cdots, n)$ are constants. With the usage of the balancing technique in Eq. (3), Eqs (4)–(6) stand as

$$u(\xi) = a_0 + a_1\mathrm{sn}^1(\xi), \tag{7}$$

$$u(\xi) = a_0 + a_1\mathrm{cn}^1(\xi), \tag{8}$$

$$u(\xi) = a_0 + a_1\mathrm{dn}^1(\xi). \tag{9}$$

2.1.1. Chirped dark and antikink solitons

Inserting Eq. (7) into Eq. (3) provides us

$$\begin{aligned} &2a_1\mathrm{sn}^3(\xi,m)m^2 - a_1\mathrm{sn}(\xi,m) + A_1a_1\mathrm{sn}(\xi,m) - a_1m^2\mathrm{sn}(\xi,m) + A_1a_0 \\ &+A_2a_0^3 + 3A_2a_0a_1^2\mathrm{sn}^2(\xi,m) + A_2a_1^3\mathrm{sn}^3(\xi,m) + 3A_2a_0^2a_1\mathrm{sn}(\xi,m) = 0 \end{aligned} \tag{10}$$

and

$$a_1\mathrm{cn}(\xi,m)\mathrm{dn}(\xi,m)(B_1 + B_2a_0^2 + 2B_2a_0a_1\mathrm{sn} + B_2a_1^2\mathrm{sn}^2(\xi,m)) = 0. \tag{11}$$

After solving Eqs (10) and (11) and gathering the coefficients of $\mathrm{sn}(\xi)$, one arrives at the following result:

$$\begin{aligned} &\mathrm{sn}^3(\xi) : 2a_1m^2 + A_2a_1^3 = 0, \\ &\mathrm{sn}^2(\xi) : 3A_2a_0a_1^2 = 0, \\ &\mathrm{sn}^1(\xi) : 3A_2a_0^2a_1 - a_1 - a_1m^2 + a_1a_1 = 0, \\ &\mathrm{sn}^0(\xi) : A_2a_0^3 + a_1a_0 = 0, \end{aligned} \tag{12}$$

and

$$\begin{aligned}
&\mathrm{sn}^2(\xi) : a_1^3 B_2 \mathrm{cndn} = 0,\\
&\mathrm{sn}^1(\xi) : 2a_1^2 B_2 a_0 \mathrm{cncn} = 0,\\
&\mathrm{sn}^0(\xi) : B_1 + B_2 a_0^2 = 0.
\end{aligned} \tag{13}$$

From the system of equations (12) and (13), we reveal

$$a_0 = \frac{\sqrt{-B_2 B_1}}{B_2}, \;\; a_1 = \frac{2m}{\sqrt{-2A_2}}. \tag{14}$$

By combining Eq. (14) with Eq. (7) and plugging them into Eq. (2), one can see the dark soliton

$$u(x,t) = \left[\frac{\sqrt{-B_2 B_1}}{B_2} + \left(\frac{2m}{\sqrt{-2A_2}}\right)\tanh(x-ct)\right]\exp\{i(\kappa x - \omega t)\}. \tag{15}$$

The dark soliton for optical fibre is depicted in Figs 1 and 2. The dark soliton can be found for $\beta = 1.1$, $\delta = 0.1$, $\Gamma = 0.000001$, $\sigma = 0.000005$, $\omega = 0.001$, $c = 0.01$ and $\kappa = 0.9$ that is visualized in Fig. 1 with the aid of the GVD (α). The dark solitonic is also portrayed in Fig. 2 with the help of the SPM (β).

With the effect of SS (δ), Eq. (15) gives the chirped dark solitonic profile by setting the parameters $\beta = 0.5$, $\alpha = 0.01$, $\Gamma = 0.1$, $\sigma = 1.5$, $\omega = 1$, $c = 5$, $\kappa = 5$ and $\delta = 0.01$, which is displayed in Fig. 3. The corresponding contour plot clearly exhibits the chirped structure in the middle region of the dark solitons (see Fig. 3a). The profile shifts from a chirped dark soliton to an antikink chirped soliton as the value of the SS coefficient ($\delta = 1$) is increased. This shift is shown in Fig. 3.

2.1.2. Chirped W-shaped bright soliton

By plugging Eq. (8) into Eq. (3), we arrive at

$$\begin{aligned}
&-a_1\mathrm{cn}(\xi,m) + 2a_1 m^2 \mathrm{dn}^2(\xi,m)\mathrm{cn}(\xi,m) + A_1 a_0 + A_1 a_1 \mathrm{cn}(\xi,m) + A_2 a_0^3\\
&+3A_2 a_0 a_1^2 + 3A_2 a_0^2 a_1 \mathrm{cn}(\xi,m) + A_2 a_1^3 \mathrm{cn}(\xi,m) - 3A_2 a_0 a_1^2 \mathrm{sn}^2(\xi,m)\\
&-A_2 a_1^3 \mathrm{sn}^2(\xi,m)\mathrm{cn}(\xi,m) = 0
\end{aligned} \tag{16}$$

and

$$\begin{aligned}
&-2a_1^2 \mathrm{sn}(\xi,m)\mathrm{dn}(\xi,m) B_2 a_0 \mathrm{cn}(\xi,m) - a_1 \mathrm{sn}(\xi,m)\mathrm{dn}(\xi,m)\Big(B_1 + B_2 a_0^2 + B_2 a_1^2\\
&-B_2 a_1^2 \mathrm{cn}^2(\xi,m)\Big) = 0,
\end{aligned} \tag{17}$$

solving Eqs (16) and (17), and by aggregating the coefficients of $\mathrm{cn}(\xi)$, one can arrive at

(a) $\alpha = 0.000001$

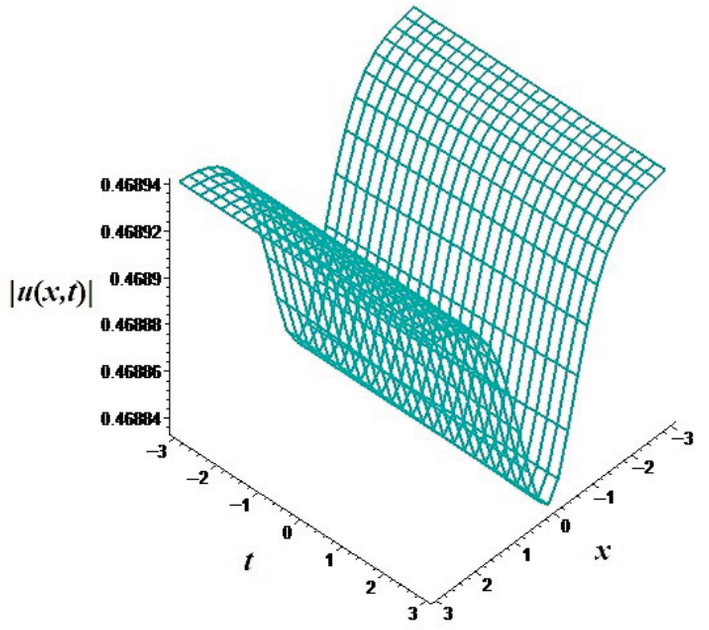

(b) $\alpha = 0.000020$

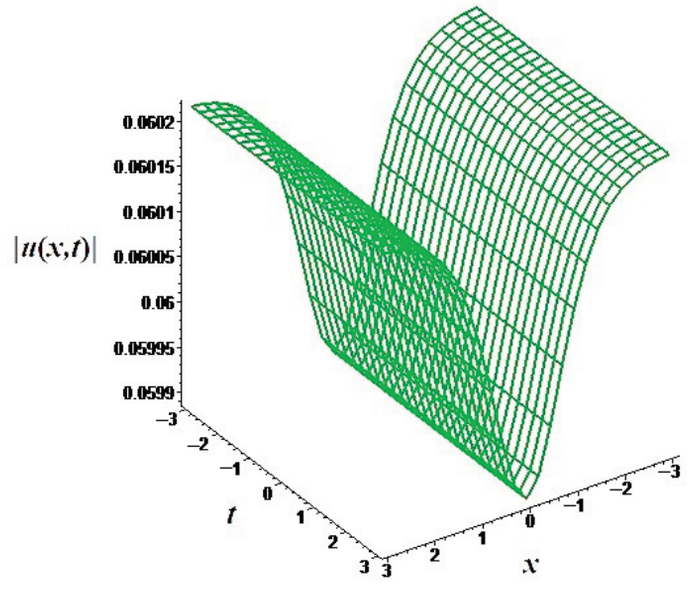

Fig. 1. Profiles of the dark soliton (15).

(a) $\beta = 1.4$

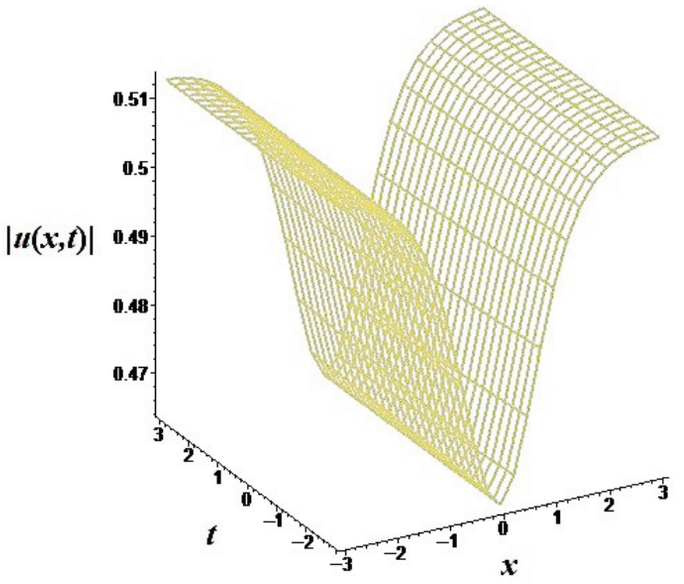

(b) $\beta = 120$

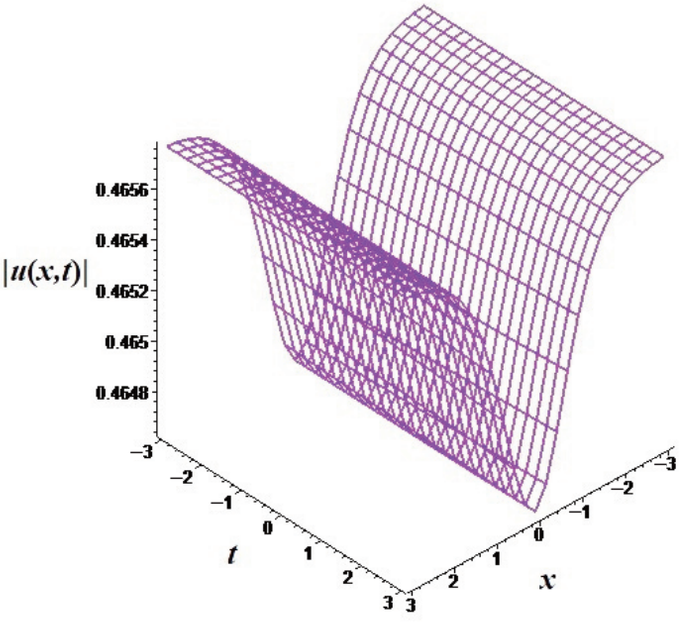

Fig. 2. Profiles of the dark soliton (15).

(a) $\delta = 0.01$

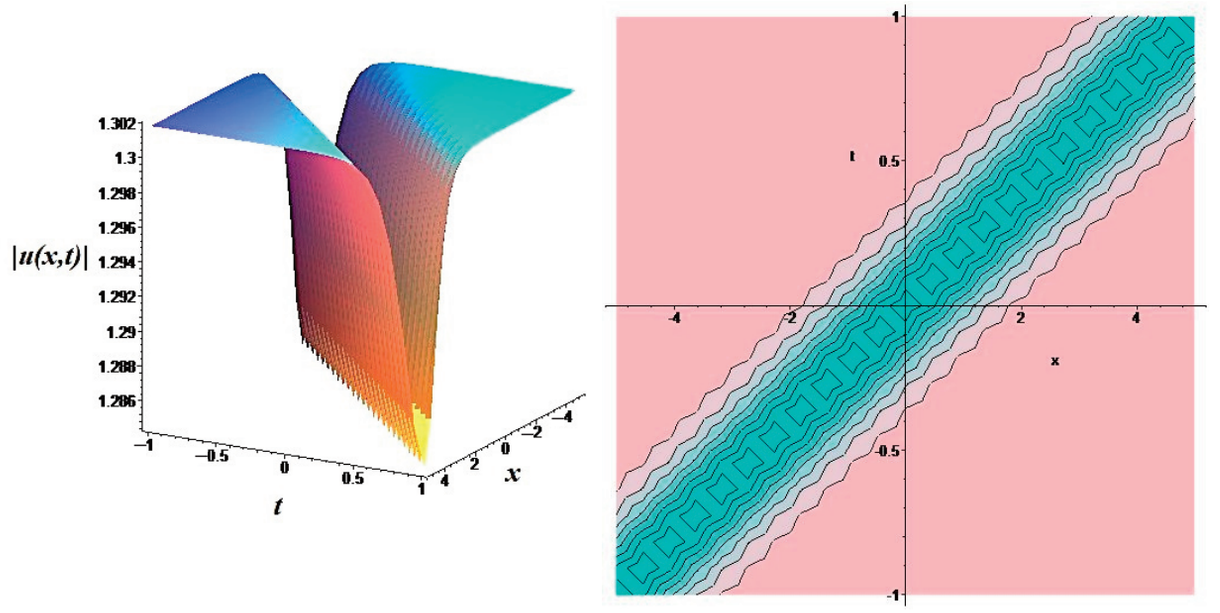

(b) $\delta = 1$

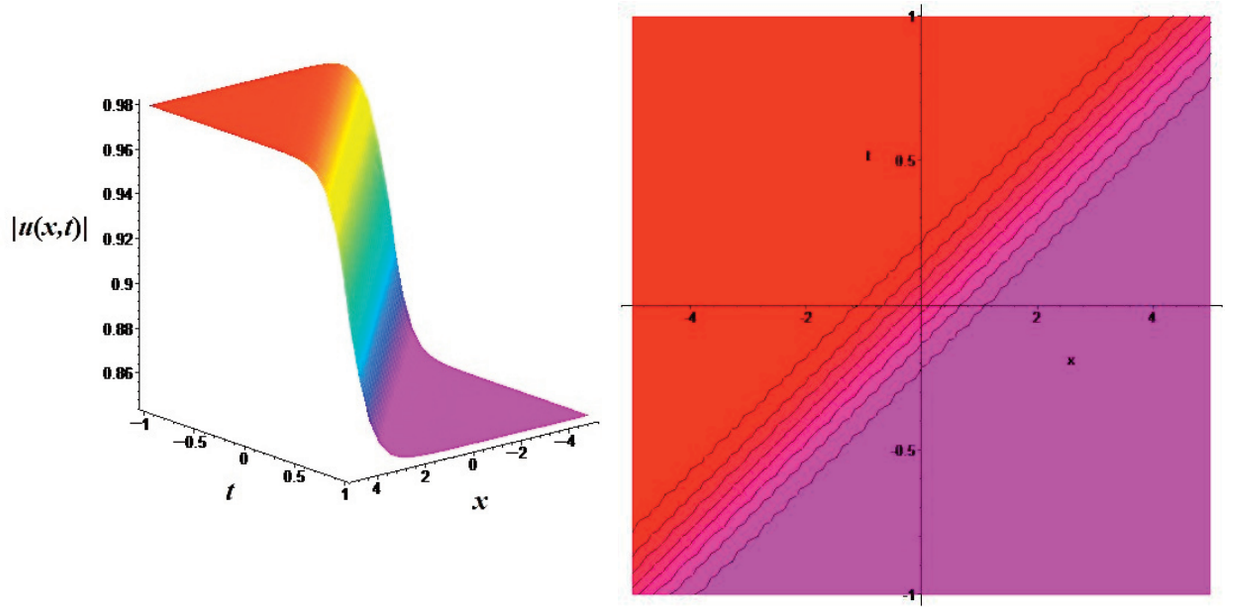

Fig. 3. Profiles of the shape-changing chirped dark soliton to antikink soliton for Eq. (15).

$$\begin{aligned}
&\mathrm{cn}^3(\xi) : A_2 a_1^3 - 2a_1 m^2 = 0,\\
&\mathrm{cn}^2(\xi) : 3A_2 a_0 a_1^2 = 0,\\
&\mathrm{cn}^1(\xi) : 2a_1 m^2 - a_1 + A_1 a_1 + 3A_2 a_0^2 a_1 = 0,\\
&\mathrm{cn}^0(\xi) : A_2 a_0^3 + A_1 a_0 = 0,
\end{aligned} \tag{18}$$

and

$$\begin{aligned}
&\mathrm{cn}^2(\xi) : B_2 a_1^2 = 0,\\
&\mathrm{cn}^1(\xi) : 2a_1^2 B_2 a_0 \mathrm{sn}(\xi,m)\mathrm{dn}(\xi,m) = 0,\\
&\mathrm{cn}^0(\xi) : B_1 + B_2 a_0^2 = 0.
\end{aligned} \tag{19}$$

From the system of equations (18) and (19), we reveal

$$a_0 = \frac{\sqrt{-B_2 B_1}}{B_2},\ a_1 = \frac{\sqrt{2}}{\sqrt{A_2} m}. \tag{20}$$

By combining Eq. (20) with Eq. (8) and plugging them into Eq. (2), one can see the bright soliton

$$u(x,t) = \left[\frac{\sqrt{-B_2 B_1}}{B_2} + \Big(\frac{\sqrt{2}}{\sqrt{A_2} m}\Big)\mathrm{sech}(x - ct)\right] \exp\{i(\kappa x - \omega t)\}. \tag{21}$$

The above equation provides the bright solitonic structure with the following parameters: $\beta = 1.1$, $\delta = 1.2$, $\Gamma = 1.0$, $\sigma = 0.5$, $\omega = 0.01$, $c = 0.01$ and $\kappa = 0.9$ that is displayed in Fig. 4 with the aid of the GVD (α). The variation of the SPM coefficient (β) also gives the bright solitonic structure, which is shown in Fig. 5.

By plotting Eq. (21), the chirped bright soliton structure changes to W-shaped chirped solitons, which is displayed in Fig. 6 under the influences of the SS coefficient (δ). In Fig. 6, both the 3d plot and the contour plot clearly visualize the chirped bright soliton profile by fixing the parameters $\beta = 0.5$, $\alpha = 10$, $\Gamma = 1$, $\sigma = 0.5$, $\omega = 1$, $c = 1$, $\kappa = 0.9$ and $\delta = 0.05$. It is interesting to note that by selecting the SS coefficient ($\delta = 1$, 10), we are able to produce the W-shaped chirped soliton profile that is illustrated in Fig. 6b,c.

2.1.3. Chirp free W-shaped bright soliton

Inserting Eq. (9) into Eq. (3) enables us

$$\begin{aligned}
&-a_1 m^2 \mathrm{dn}(\xi,m) + 2a_1 m^2 \mathrm{sn}^2(\xi,m)\mathrm{dn}(\xi,m) + A_1 a_1 \mathrm{dn}(\xi,m) + A_1 a_0\\
&+3A_2 a_0^2 a_1 \mathrm{dn}(\xi,m) + A_2 a_0^3 - 3A_2 a_0 a_1^2 m^2 \mathrm{sn}^2(\xi,m) + 3A_2 a_0 a_1^2\\
&-A_2 a_1^3 m^2 \mathrm{sn}^2(\xi,m)\mathrm{dn}(\xi,m) + A_2 a_1^3 \mathrm{dn}(\xi,m) = 0
\end{aligned} \tag{22}$$

(a) $\alpha = 0.000001$

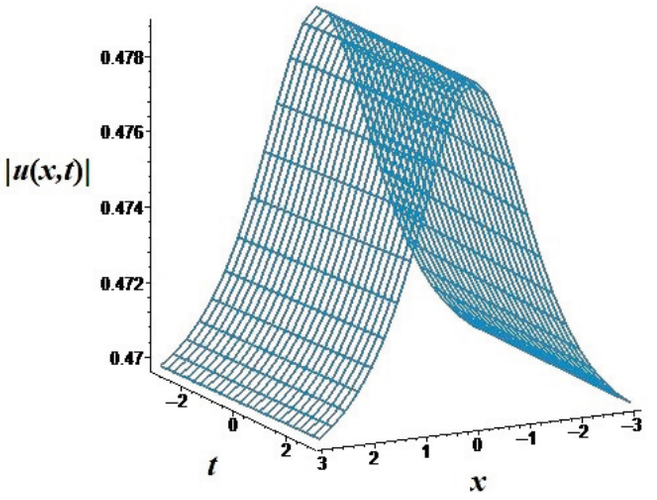

(b) $\alpha = 0.00001$

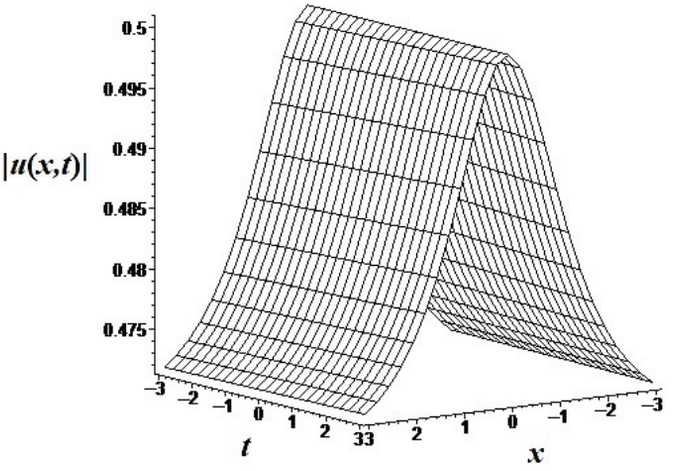

Fig. 4. Profiles of the bright soliton (21).

(a) $\beta = 0.01$

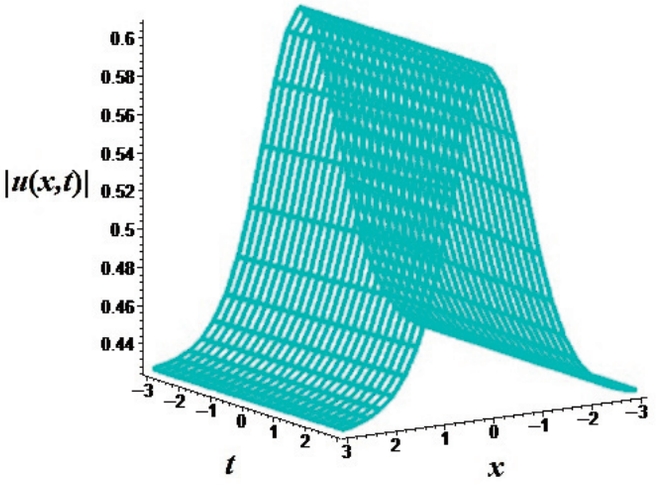

(b) $\beta = 10$

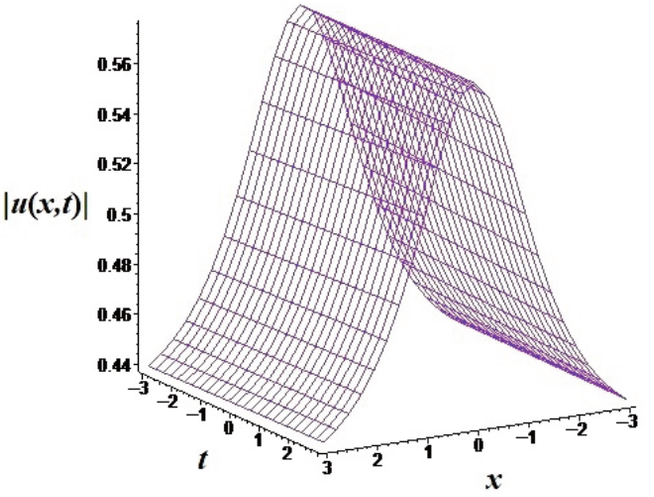

Fig. 5. Profiles of the bright soliton (21).

(a) $\delta = 0.05$

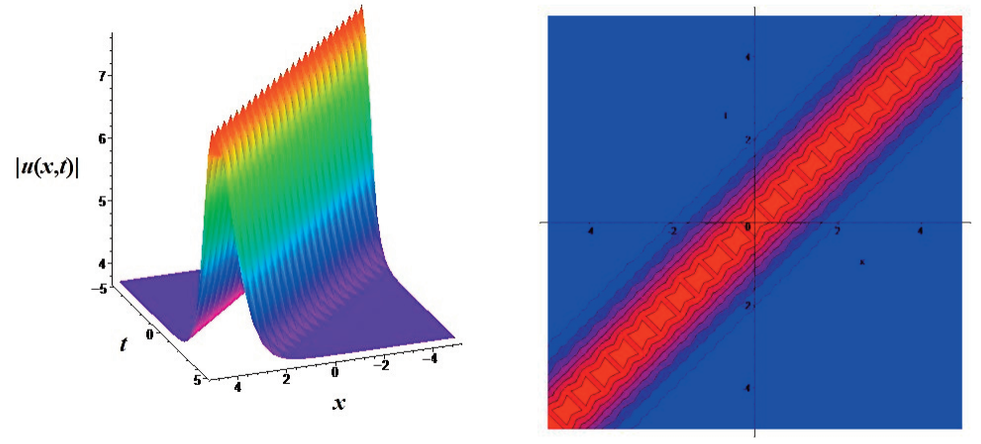

(b) $\delta = 1$

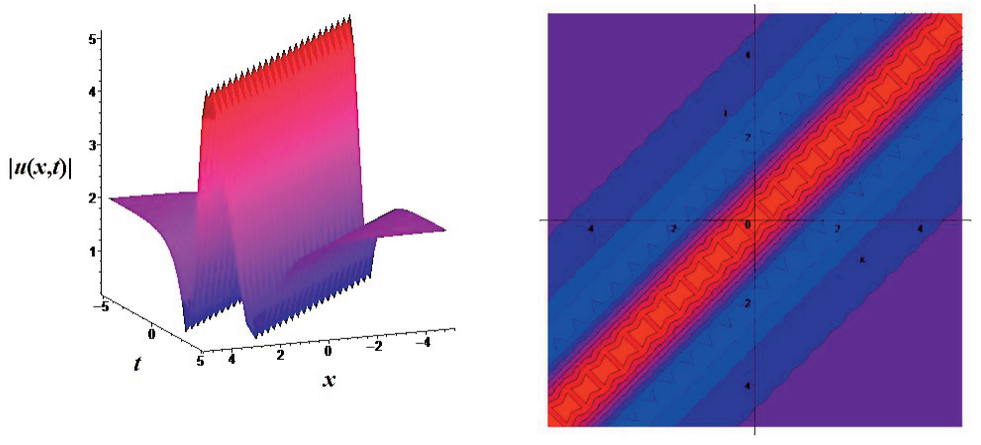

(c) $\delta = 10$

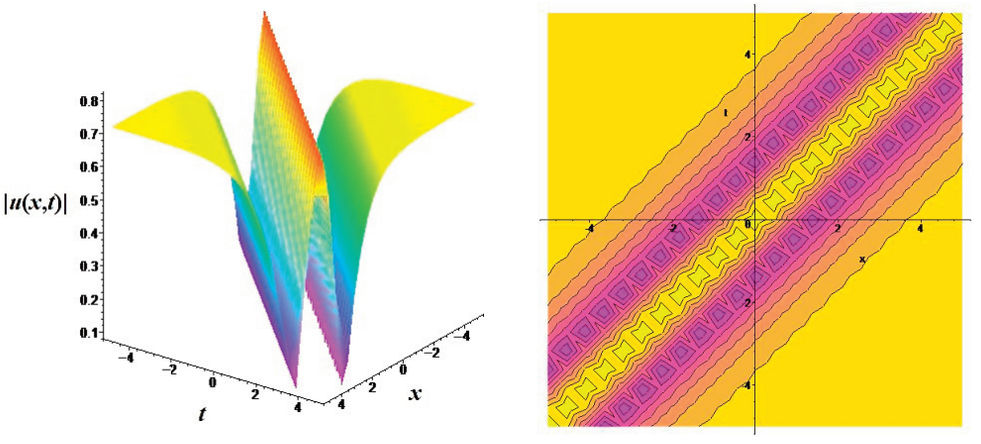

Fig. 6. Profiles of the *W*-shaped chirped soliton (21).

and

$$-2a_1^2\mathrm{cn}(\xi,m)\mathrm{sn}(\xi,m)B_2a_0\mathrm{dn}(\xi,m)-a_1\mathrm{sn}(\xi,m)\mathrm{dn}(\xi,m)\Big(B_1+B_2a_0^2+B_2a_1^2 -B_2a_1^2\mathrm{sn}(\xi,m)^2\Big)=0, \tag{23}$$

solving Eqs (22) and (23), and by accumulating the coefficients of $\mathrm{cn}(\xi)$, one is able to obtain

$$\begin{aligned}
&\mathrm{dn}^3(\xi):-2a_1+A_2a_1^3=0,\\
&\mathrm{dn}^2(\xi):3A_2a_0a_1^2=0,\\
&\mathrm{dn}^1(\xi):-a_1m^2+2a_1+3A_2a_0^2a_1+A_1a_1=0,\\
&\mathrm{dn}^0(\xi):A_2a_0^3+A_1a_0=0,
\end{aligned} \tag{24}$$

and

$$\begin{aligned}
&\mathrm{dn}^5(\xi):a_1^3B_2\mathrm{sn}(\xi,m)=0,\\
&\mathrm{dn}^3(\xi):-2a_1^3B_2\mathrm{sn}(\xi,m)=0,\\
&\mathrm{dn}^1(\xi):\frac{a_1^3\mathrm{sn}(\xi,m)B_2}{m^4}-a_1^3\mathrm{sn}(\xi,m)B_2-2a_1^2\mathrm{cn}(\xi,m)B_2a_0\mathrm{sn}(\xi,m)\\
&-a_1B_1\mathrm{sn}(\xi,m)-a_1B_2a_0^2\mathrm{sn}(\xi,m)=0.
\end{aligned} \tag{25}$$

From the system of equations (24) and (25), we reveal

$$\begin{aligned}
a_0&=-\frac{a_1B_2\mathrm{cn}(\xi,m)m^2-\sqrt{a_1^2B_2^2\mathrm{cn}^2(\xi,m)m^4+a_1^2B_2^2-a_1^2B_2^2m^4-B_2m^4B_1}}{B_2m^2},\\
a_1&=\frac{\sqrt{2}}{\sqrt{A_2}}.
\end{aligned} \tag{26}$$

By combining Eq. (26) and Eq. (9), and then entering them into Eq. (2), one may see the bright soliton

$$u(x,t)=\left[-\frac{a_1B_2\mathrm{cn}(\xi,m)m^2-\sqrt{a_1^2B_2^2\mathrm{cn}^2(\xi,m)m^4+a_1^2B_2^2-a_1^2B_2^2m^4-B_2m^4B_1}}{B_2m^2} +\left(\frac{\sqrt{2}}{\sqrt{A_2}}\right)\mathrm{sech}(x-ct)\right]\exp\{i(\kappa x-\omega t)\}. \tag{27}$$

The bright soliton for optical fibre is represented by the equation that was stated in Figs 7 and 8. By setting the parametric values $\beta=1.1$, $\delta=1.2$, $\Gamma=1.0$, $\sigma=0.5$, $\omega=0.01$, $c=0.01$ and $\kappa=0.9$, we obtain the bright solitonic for $\alpha=0.000001$ that is plotted in Fig. 7a. The amplitude of the bright solitonic structure is increasing with the help of $\alpha=0.00001$ that is depicted in Fig. 7b. Under the influences of the coefficient SPM (β), we obtain the shape changing property from dark solitonic structure to bright solitonic structure with $\alpha=0.1$, $\delta=1.2$, $\Gamma=1.0$, $\sigma=0.5$, $\omega=0.01$, $c=0.01$ and $\kappa=0.9$, which is depicted in Fig. 8.

(a) $\alpha = 0.000001$

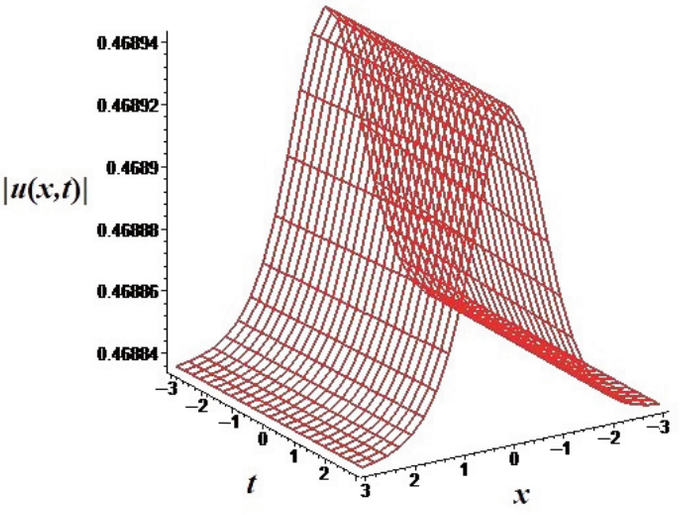

(b) $\alpha = 0.00001$

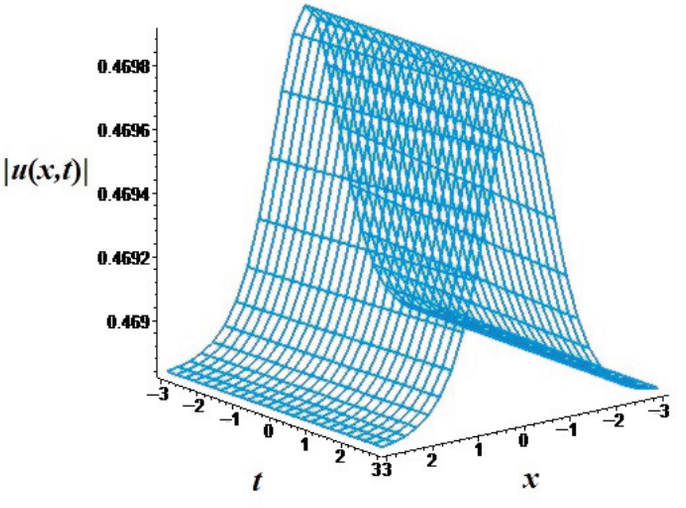

Fig. 7. Profiles of the bright soliton (27).

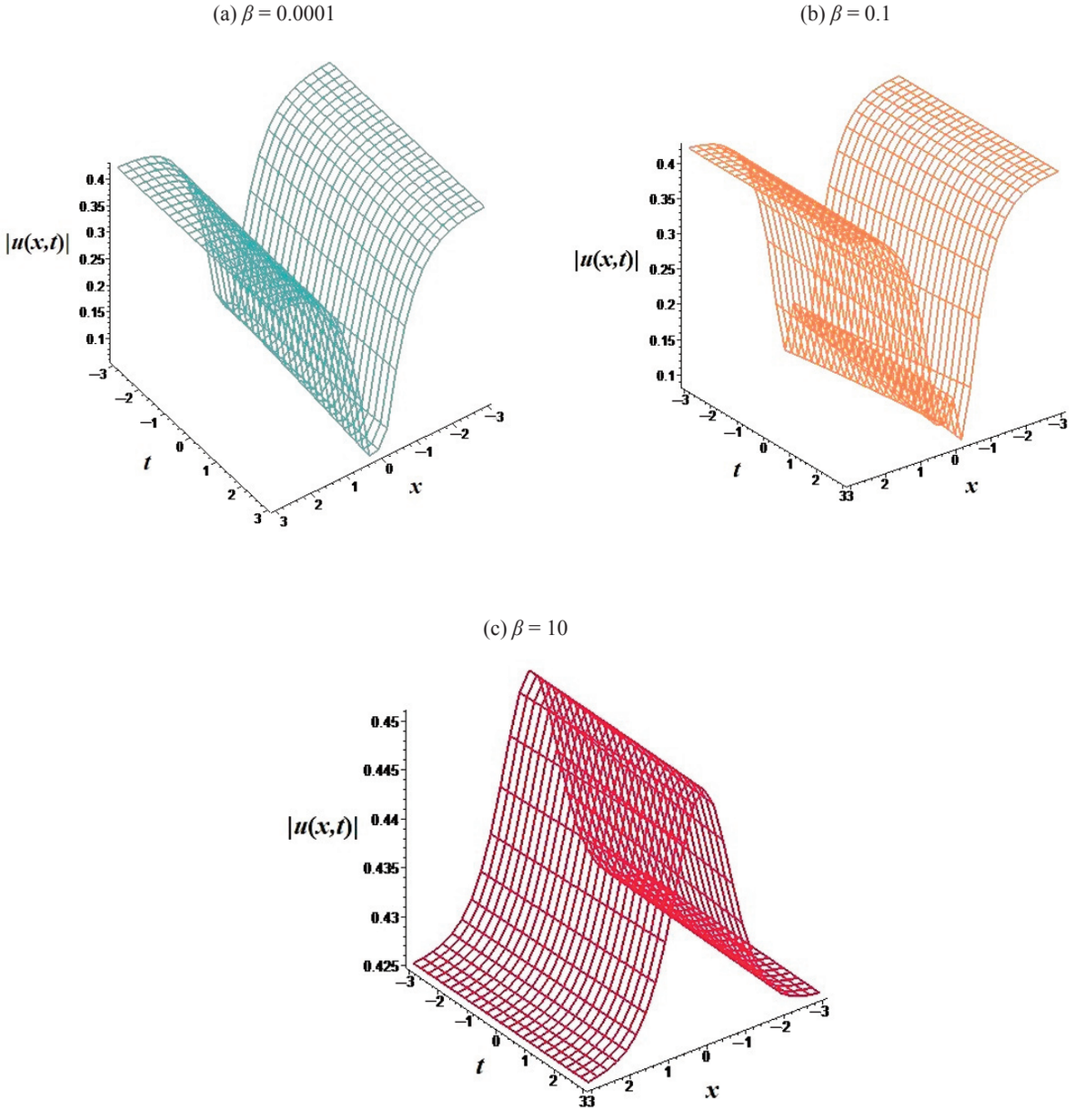

Fig. 8. Profiles of the shape-changing one dark soliton to one bright soliton for Eq. (27).

Eq. (27) also provides the chirp free soliton profile and the W-shaped chirp free soliton profile when dominating the SS coefficient (δ), which is displayed in Fig. 9 that shows the chirp free bright soliton profile (for $\delta = 1$) by choosing $\alpha = 10$, $\beta = 0.5$, $\Gamma = 0.7$, $\sigma = 0.5$, $\omega = 0.1$, $c = 0.001$ and $\kappa = 0.9$. The chirp free bright soliton changes its profile to W-shaped chirp free soliton when $\delta = 0.1, 0.05$, which is given in Fig. 9b,c.

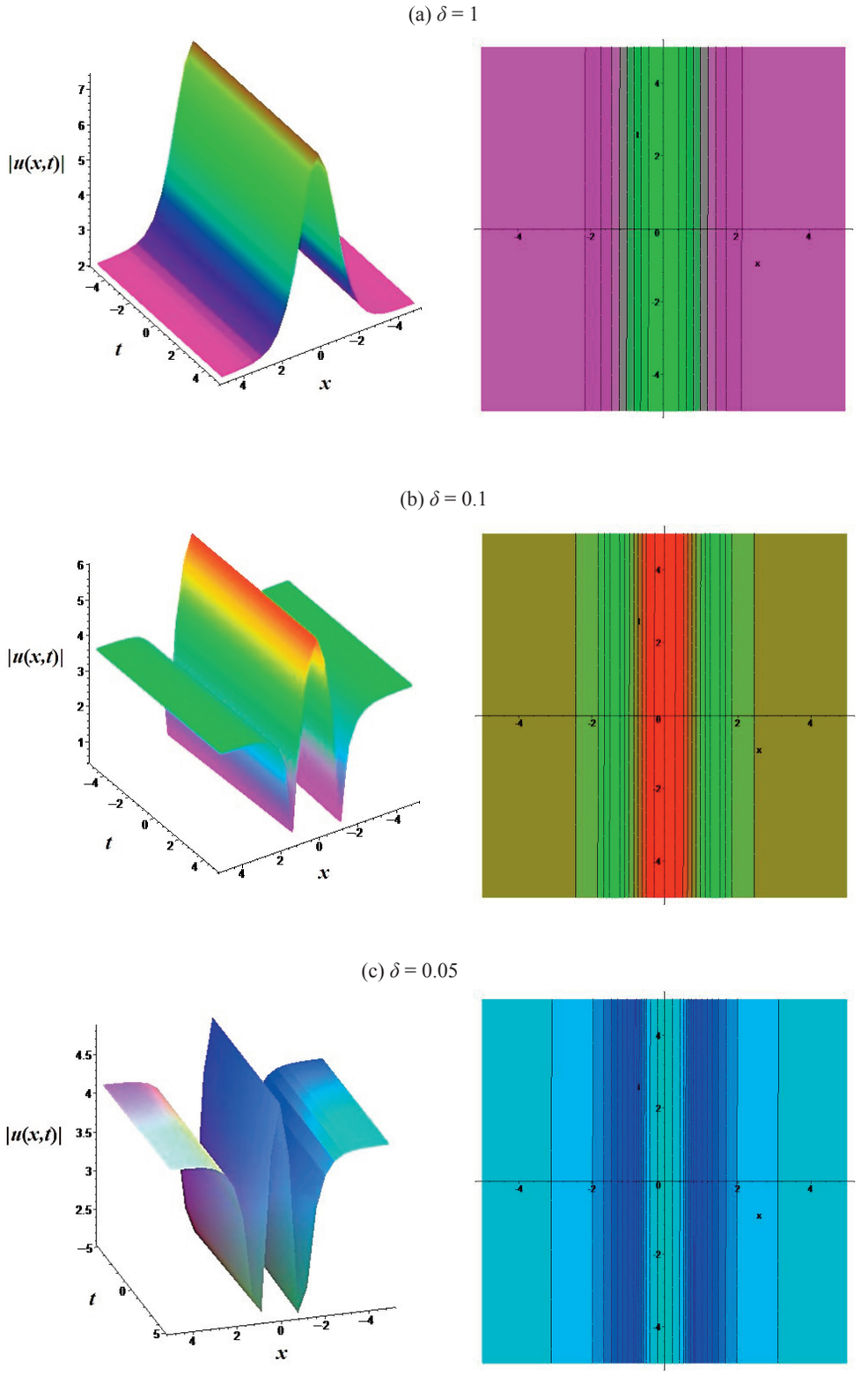

Fig. 9. Profiles of the *W*-shaped chirp free soliton (27).

3. CONCLUSIONS

We report the exact W-shaped bright and dark solitons (both chirped & chirp free solitons) for perturbed NLSE using the JEF algorithm. Soliton solutions for the NLSE, which is an essential component for assessing pulse propagation in optical fiber-based communications systems, are required. Therefore, based on the present effective algorithm, we have successfully obtained the W-shaped dark, bright soliton solutions for dn(ξ), cn(ξ) and sn(ξ) functions when $m \to 1$. (If we choose $m \to 0$, we obviously obtain trigonometry structures). Moreover, the current algorithm is straightforward and very simple to acquire soliton solutions, and it can be modeled to solve other similar NLPDEs.

In the case of sn(ξ), the effect of the GVD coefficient (α) causes the amplitude of the dark solitonic profile to drop when the value of α is increased. Additionally, the two wing parts move closer to one another, which results in a shortening of the wing. When the value of the nonlinear coefficient β is increased, the profile shifts from shortening to broadening, and the amplitude of the profiles drops. In other words, β is a nonlinear coefficient. The SS coefficient (δ) presents the shape changing property from chirped dark soliton to chirped antikink soliton structure with amplitude decrements when δ increases. In cn(ξ) for the GVD coefficient, the amplitude of the profiles decreases by increasing the value of the SPM coefficient (β), while the amplitude of the profiles increases by increasing the value of α. By increasing the value of the SS coefficient (δ), the amplitude of the chirped soliton decreases. Particularly, the middle region of the chirped soliton heavily decreases and the wing portions are also decreased by increasing the value of δ (see Fig. 6b,c). For dn(ξ) under the effect of the GVD coefficient, the amplitude of the profiles increases by increasing the values of α, but the SPM coefficient influences the shape changing property from dark soliton to bright soliton. The middle region of the dark soliton slightly moves in the upward direction, while the wing portions move downward under the influences of the coefficient of SPM. When δ decreases, the amplitude of the W-shaped chirp free solitons, as well as the middle region of the chirped soliton decrease. By decreasing the value of δ (see Fig. 9b,c), the wing portions increase.

The generation of a chirped soliton profile can be attributed, in its most basic form, to a balance between the SS effects and GVD, correspondingly. Many researchers have found W-shaped solitons under the influences of GVD, SS, and SPM. The observation of the W-shaped chirped and chirp free solitons is one of the fundamental findings in the current paper. Also, antikink solutions are retrieved to secure in this optical system specific values of the SS coefficient in the sn(ξ) function. The efficiency of the JEF integration algorithm is displayed by the sn(ξ) function, which depicts dark solitons as a result of the influence of the GVD and SPM coefficients, in addition to chirped dark solitons and antikink solitons, which are created by the SS coefficient. Obviously, the cn(ξ) and dn(ξ) functions give the bright solitonic profile. Subsequently, the chirped W-shaped solitons are generated by the cn(ξ) function, but the dn(ξ) function generates the chirp-free W-shaped solitons. From the above discussion, we concluded that by compressing or shortening the solitonic structure with GVD, we received the previously known result, i.e. decreasing of the solitonic profile duration in the femtosecond, or ultrashort region. Subsequently, broadening of the soliton profile with a coefficient of SPM provides known information, i.e. the propagation of high-intensity femtosecond solitons. Moreover, shortening/compressing of the soliton profile with the SPM coefficient provides the loss of energy during propagation.

ACKNOWLEDGEMENTS

Annamalai Muniyappan gratefully acknowledges the Theivanai Ammal College for Women (A), Villupuram, Tamilnadu, India for providing the DST-FIST lab. The publication costs of this article were partially covered by the Estonian Academy of Sciences.

REFERENCES

1. Mollenauer, L. F., Stolen, R. H. and Gordon, J. P. Experimental observation of picosecond pulse narrowing and solitons in optical fibers. *Phys. Rev. Lett.*, 1980, **45**, 1095.
2. Malomed, B. A. Ideal amplification of an ultrashort soliton in a dispersion-decreasing fiber. *Opt. Lett.*, 1994, **19**, 341.
3. Liu, W. Parallel line rogue waves of a (2+1)-dimensional nonlinear Schrödinger equation describing the Heisenberg ferromagnetic spin chain. *Romanian J. Phys.*, 2017, **62**, 1–16.
4. Muniyappan, A., Sharon L. N. and Suruthi, A. Excitations of periodic kink breathers and dark/bright breathers in a microtubulin protofilament lattices. *Nonlinear Dyn.*, 2021, **106**, 3495–3506.
5. Wazwaz, A. M. A sine-cosine method for handling nonlinear wave equations. *Math. Comput. Model.*, 2004, **40**, 499–508.
6. Akram, G., Arshed, S. and Imran, Z. Soliton solutions for fractional DNA Peyrard–Bishop equation via the extended $(\frac{G'}{G^2})$-expansion method. *Physica Scr.*, 2021, **96**, 094009.
7. Biswas, A., Jawad, A. J. M., Manrakhan, W. N., Sarma, A. K. and Khan, K. R. Optical solitons and complexitons of the Schrödinger–Hirota equation. *Opt. Laser Technol.*, 2012, **44**(7), 2265–2269.
8. Rezazadeh, H., Ullah, N., Akinyemi, L., Shah, A., Mirhosseini-Alizamin, S. M., Chu, Y. M. and Ahmad, H. Optical soliton solutions of the generalized non-autonomous nonlinear Schrödinger equations by the new Kudryashov's method. *Results Phys.*, 2021, **24**, 104179.
9. Akinyemi, L., Senol, M., Mirzazadeh, M. and Eslami, M. Optical solitons for weakly nonlocal Schrödinger equation with parabolic law nonlinearity and external potential. *Optik*, 2021, **230**, 166281.
10. Radha, R. and Lakshmanan, M. Singularity structure analysis and bilinear form of a (2 + 1) dimensional non-linear Schrödinger (NLS) equation. *Inverse Problems*, 1994, **10**, 29–32.
11. Biswas, A., Rezazadeh, H., Mirzazadeh, M., Eslami, M., Zhou, Q., Moshokoa, S. P. and Belic, M. Optical solitons having weak non-local nonlinearity by two integration schemes. *Optik*, 2018, **164**, 380–384.
12. Zhou, Q., Liu, L., Zhang, H., Mirzazadeh, M., Bhrawy, A. H., Zerrad, E. et al. Dark and singular optical solitons with competing nonlocal nonlinearities. *Opt. Appl.*, 2016, **46**, 79–86.
13. Wazwaz, A. M. Multiple-soliton solutions of two extended model equations for shallow water waves. *Appl. Math. Comput.*, 2008, **201**, 790–799.
14. Sakaguchi, H. and Malomed, B. A. Gross–Pitaevskii–Poisson model for an ultracold plasma: Density waves and solitons. *Phys. Rev. Research*, 2020, **2**, 033188.
15. Muniyappan, A., Sahasraari, L. N., Anitha, S., Ilakiya, S., Biswas, A., Yıldırım, Y. et al. Family of optical solitons for perturbed Fokas–Lenells equation. *Optik*, 2022, **249**, 168224.
16. Biswas, A. and Milovic, D. Bright and dark solitons of the generalized nonlinear Schrödinger's equation. *Commun. Nonlinear Sci. Numer. Simul.*, 2010, **15**, 1473–1484.
17. Muniyappan, A., Monisha, P., Priya, E. K. and Nivetha, V. Generation of wing-shaped dark soliton for perturbed Gerdjikov–Ivanov equation in optical fibre. *Optik*, 2021, **230**, 166328.
18. Kivshar, Y. S. and Agrawal, G. P. *Optical Solitons: From Fibers to Photonic Crystals*. Academic Press, San Diego, California, 2003.
19. Goyal, A., Gupta, R., Kumar, C. N. and Raju, T. S. Chirped femtosecond solitons and double-kink solitons in the cubic-quintic nonlinear Schrödinger equation with self-steepening and self-frequency shift. *Phys. Rev. A*, 2011, **84**, 063830.
20. Vyas, V. M., Patel, P., Panigrahi, P. K., Kumar, C. N. and Greiner, W. Chirped chiral solitons in the nonlinear Schrödinger equation with self-steepening and self-frequency shift. *Phys. Rev. A*, 2008, **78**, 021803(R).
21. Kumar, C. N. and Durganandini, P. New phase modulated solutions for a higher-order nonlinear Schrödinger equation. *Pramana J. Phys.*, 1999, **53**, 271.
22. Triki, H., Biswas, A., Milovic, D. and Belic, M. Chirped femtosecond pulses in the higher-order nonlinear Schrödinger equation with non-Kerr nonlinear terms and cubic-quintic-septic nonlinearities. *Opt. Commun.*, 2016, **366**, 362–369.
23. Triki, H., Porsezian, K. and Grelu, P. Chirped soliton solutions for the generalized nonlinear Schrödinger equation with polynomial nonlinearity and non-Kerr terms of arbitrary order. *J. Opt.*, 2016, **18**, 075504.
24. Triki, H., Porsezian, K., Choudhuri, A. and Dinda, P. T. Chirped solitary pulses for a nonic nonlinear Schrödinger equation on a continuous-wave background. *Phys. Rev. A*, 2016, **93**, 063810.
25. Desaix, M., Helczynski, L., Anderson, D. and Lisak, M. Propagation properties of chirped soliton pulses in optical nonlinear Kerr media. *Phys. Rev. E*, 2002, **65**, 056602.